

PAPERS | JULY 01 2021

Hysteresis in a simple V-shaped spring-mass system

Christopher Ong



Am. J. Phys. 89, 663–665 (2021)
<https://doi.org/10.1119/10.0003536>



Special Topic:
Teaching about the environment,
sustainability, and climate change

AAPT
PHYSICS EDUCATION[®]

Read Now

Hysteresis in a simple V-shaped spring-mass system

Christopher Ong^{a)}

106B Faber Drive, Singapore 129416

(Received 24 December 2020; accepted 27 January 2021)

This paper theoretically studies a simple system of two identical linear springs connected symmetrically to a mass in a V-shaped configuration, with an additional adjustable external force applied to the mass. As this force is varied, under certain conditions the equilibrium position of the mass demonstrates strong dependence on the history of changes in the external force, exhibiting hysteresis. Mathematically, variations of the external force cause the system to undergo two saddle-node bifurcations at two differing critical points, leading separately to the creation and destruction of branches of stable equilibria. Analysis of the bifurcation diagram shows that the saddle-node bifurcations cause hysteresis in the system, and the behavior is summarized in a hysteresis graph. © 2021 Published under an exclusive license by American Association of Physics Teachers.

<https://doi.org/10.1119/10.0003536>

I. INTRODUCTION

Hysteresis is a nonlinear phenomenon, in which the behavior of a system depends on its history. This is in direct contrast to most ordinary physical systems, whose behavior can be uniquely predicted based solely on their current state. Standard undergraduate laboratory experiments aimed at demonstrating hysteresis are typically restricted¹ to ferroelastics, in which hysteresis arises from the deformation of nonlinear elastic materials,²⁻⁴ or ferromagnets, where the alignment of magnetic domains in response to an external magnetic field gives rise to hysteresis.⁵⁻⁷ There are also mechanical illustrations of hysteresis using driven pendulums⁸⁻¹⁰ and driven Duffing oscillators.^{11,12} However, the setups for these demonstrations are convoluted and obscure, often requiring unfamiliar types of materials. From a pedagogical standpoint, it is difficult to develop an intuitive feel for the sources of hysteresis in such systems. This also creates the impression that hysteresis-related phenomena are rare in nature, and that hysteresis only appears in specific fringe cases with materials that exhibit uncommon properties.

In this paper, we present the analytic theory of a remarkably simple mechanical system that unexpectedly demonstrates hysteresis. It only consists of two ordinary springs and a mass. Given that the average person has experience with springs and gravity on a daily basis, the source of hysteresis is easy to understand, and its physical significance is very clear. The occurrence of hysteretic effects despite the sheer simplicity of the setup simultaneously highlights the fact that hysteresis can arise in all kinds of systems, and is potentially more common than one might expect. We invite experimentalists to design and build a demonstration apparatus based on this analysis.

II. SETUP

The system consists of two identical springs that are each connected to the same mass at one end, and symmetrically fixed to an attachment point at its other end, forming a V-shaped spring configuration as shown in Fig. 1. The springs are idealized and assumed to have linear elastic properties, so that they obey Hooke's Law. Besides the forces from the springs, a controllable vertical external force is applied to the mass. In an actual apparatus, this force could

be adjusted using, for example, an attached weight hanger with variable slotted masses.

We denote this external force as f , and include the weight of the mass as part of f . We also denote the spring constant of each spring as k . As shown in Fig. 1, distance x is defined as half of the horizontal distance between the two attachment points of the two springs, while y is the vertical displacement of the mass below the horizontal line that passes through the springs' attachment points. The downward direction is taken to be positive for both f and y . Finally, l_0 represents the relaxed length of each spring.

Adding the external force f to the vertical component of the force exerted by both springs, we can obtain an expression for F , the net vertical force acting on the mass

$$F(y) = f - 2ky \left(1 - \frac{l_0}{\sqrt{x^2 + y^2}} \right), \quad (1)$$

with the downward direction taken to be positive.

Let us consider the graph of $F(y)$ shown in Fig. 2. From Eq. (1), we can see that f imparts a vertical shift to the shape of the entire graph. There are two qualitatively distinct sketches for the case (a) $l_0 < x$ and (b) $l_0 > x$, corresponding to whether the springs are extended or compressed at $y = 0$. Of particular interest are the values of y^* for which $F(y^*) = 0$, which physically represent the equilibrium positions of the mass. In the former case (a), there is only one

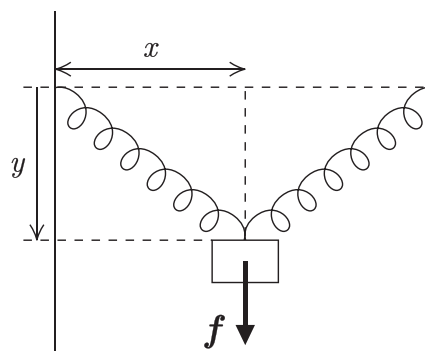


Fig. 1. Labeled diagram of the system. A typical position of the mass for $y > 0$ is shown, where the springs form a V-shape. An alternative $y < 0$ position is also possible, which gives an inverted V-shaped configuration.

value of y^* for a given value of f . This is unsurprising, since $l_0 < x$ means that the springs are in the state of extension for all y , so there is only a single y^* where the spring forces have just the right upward component to balance the external force. On the other hand, the latter case (b) can produce up to three values of y^* . This is plausible, since for $l_0 > x$, the spring will be compressed for some values of y , and extended for others; hence there may be several values of y^* corresponding to different states of the springs.

In fact, the variation of l_0 results in a supercritical pitchfork bifurcation at $l_0 = x$, but this will not be a focus in the remaining investigation.

III. BIFURCATION STUDY

From this point onward, we will choose l_0 such that $l_0 > x$, and study how y^* changes with f . It is important to note that we change f slowly and in a quasi-static manner, such that each change in f is preceded by a sufficiently long period for the system to settle to rest at a state of equilibrium.

Let us first consider how the number of solutions of y^* changes with f . As implied in Eq. (1), increasing f produces an upward translation of the graph of $F(y)$. This is illustrated in Fig. 3. Starting with a very negative value of f (Fig. 3(i)), there is only one value of y^* . Because $F'(y^*) < 0$, y^* must be a stable equilibrium point. To see this, imagine perturbing the mass upward from its equilibrium position such that $y < y^*$. Then $F(y < y^*) > 0$, indicating that the net force produced is downward, restoring the mass to its original y^* . Conversely, if the mass is perturbed in the downward direction, $F(y > y^*) < 0$, so the resultant force is now upward, and the mass again returns to y^* . (The mass may execute some oscillations in its transient motion, but it will ultimately settle at y^* after the oscillations are damped out.)

As f becomes less negative, a new value of y^* appears at the critical value $f=f_1$ (Fig. 3(ii)). This is the onset of a saddle-node bifurcation. Further increasing f (Fig. 3(iii)) produces yet another y^* , or three values of y^* in total. Considering the slope of $F(y)$ at each y^* , the smallest and largest y^* are both stable equilibrium points, whereas the central y^* value is unstable. Another saddle-node bifurcation occurs at the next critical value $f=f_2$ (Fig. 3(iv)). Here, the originally central y^* and the leftmost y^* merge together, forming a single y^* value. Beyond $f=f_2$, the merged y^* vanishes (Fig. 3(v)), leaving behind only one y^* that is a stable equilibrium position.

We can determine the two critical values f_1 and f_2 . Notice that at $f=f_1$, the local maximum lies on the horizontal axis, whereas at $f=f_2$, the local minimum lies on the horizontal axis. To find each of these turning points, we impose the

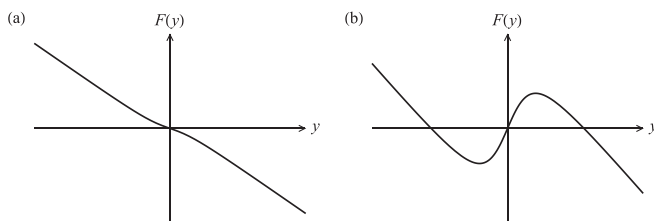


Fig. 2. $F(y)$ for (a) $l_0 < x$, (b) $l_0 > x$ and $f=0$. There is significant qualitative difference in the shapes of the two graphs and the number of y^* values, where $F(y^*) = 0$.

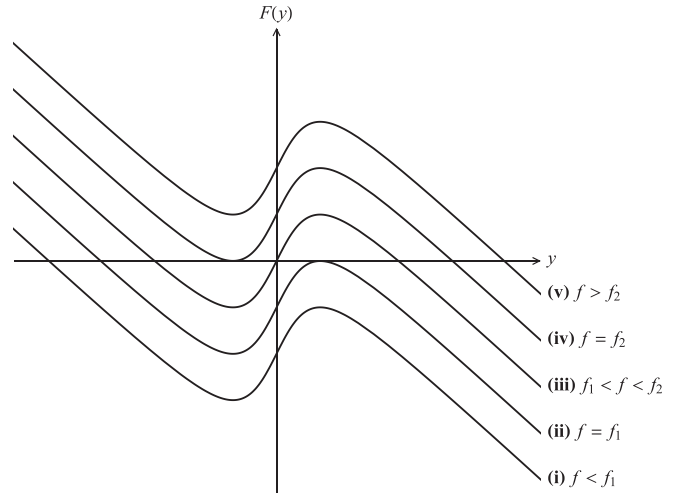


Fig. 3. $F(y)$ as f is increased, from (i) $f < f_1$, (ii) $f=f_1$, (iii) $f_1 < f < f_2$, (iv) $f=f_2$, and finally (v) $f > f_2$. The number of equilibrium positions y^* changes with f , with differing stability properties.

condition $F'(y) = 0$. Solving for y then gives the values of y at each of these turning points

$$y = \pm \sqrt{l_0^{2/3} x^{4/3} - x^2}. \quad (2)$$

As a check, note that these values of y are real if and only if $l_0 > x$. The corresponding values of F_{\min} at the minima [using the $y < 0$ solution from Eq. (2)] and F_{\max} at the maxima ($y > 0$) can then be evaluated:

$$F_{\min} = f - 2k \sqrt{l_0^{2/3} x^{4/3} - x^2} \left[\left(\frac{l_0}{x} \right)^{2/3} - 1 \right], \quad (3)$$

$$F_{\max} = f + 2k \sqrt{l_0^{2/3} x^{4/3} - x^2} \left[\left(\frac{l_0}{x} \right)^{2/3} - 1 \right]. \quad (4)$$

Now we impose the conditions that $F_{\max} = 0$ when $f=f_1$, and that $F_{\min} = 0$ when $f=f_2$, as previously discussed. These conditions enable us to find f_1 and f_2 ,

$$f_1 = -f_2 = -2k \sqrt{l_0^{2/3} x^{4/3} - x^2} \left[\left(\frac{l_0}{x} \right)^{2/3} - 1 \right]. \quad (5)$$

Putting this all together, we can visualize how y^* changes with f through the bifurcation diagram plotted in Fig. 4. Evidently, for $f < f_1$, only the lower branch of stable equilibria exists, where $y^* < 0$. In the range $f_1 < f < f_2$, the lower and upper stable branches co-exist, with an unstable central branch. For $f > f_2$, the lower stable branch and unstable central branch both vanish, leaving behind the upper stable branch. This agrees with our prior analysis of the changes in the graph of $F(y)$, when f is increased (Fig. 3). It can also be seen that within $f_1 < f < f_2$, where there exist two branches of stable equilibria, the springs are extended in one of the equilibrium positions and compressed in the other.

IV. HYSTERESIS

From the bifurcation diagram in Fig. 4, we deduce that the equilibrium position of the mass exhibits hysteretic effects as

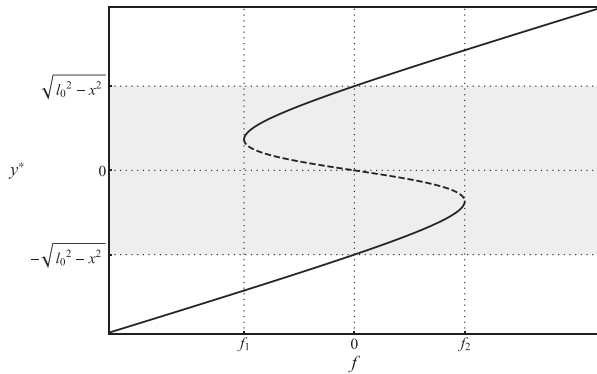


Fig. 4. Bifurcation diagram showing the changes in y^* as f is varied. This was generated by numerically solving $F(y^*) = 0$ for y^* at every value of f . The solid lines represent branches of stable equilibria, whereas the dashed line represents the unstable equilibria. The shaded region showcases the values of y^* for which the springs are in a state of compression. Outside of this region, the springs are extended.

f is varied. Imagine starting out at $f < f_1$, so that the state of the system initially lies on the lower stable branch. If we now increase f until $f_1 < f < f_2$, even though there now exist two other possible branches of y^* , the system will remain on the lower stable branch. This is characteristic of a stable equilibrium point, which draws the system to remain in its vicinity. When $f > f_2$, the lower stable branch disappears, forcing the mass to position itself on the upper stable branch. If we now lower f back to the region $f_1 < f < f_2$, rather than returning to the lower stable branch, the system instead tends to stay on the upper stable branch. The system only returns to the lower stable branch when $f < f_1$. This is a direct illustration of hysteresis, since, depending on the history of the system (particularly whether f was originally smaller than f_1 or larger than f_2), the behavior of the system differs greatly in the region $f_1 < f < f_2$. This is illustrated more clearly in Fig. 5.

To physically visualize how the system would behave, notice that $y^* > 0$ means the springs have a V-shaped configuration, whereas $y^* < 0$ means the springs have an inverted V-shaped configuration. In essence, the physical significance of hysteresis is that switching from an inverted V to a V requires $f > f_2$, whereas switching from V back to inverted V requires $f < f_1$. Intuitively, this means that the spring configuration consistently “prefers” to retain its original shape, and forcing it to invert its shape requires a higher-than-expected force. Moreover, when the critical values f_1 and f_2 are reached, the inversion of the springs’ configuration results in a sudden drastic change in y^* . Simultaneously, the springs switch between being compressed and being extended.

V. CONCLUSION

Contrary to popular belief, hysteresis can show up in even the simplest systems, such as the mechanical system analyzed in this study. Under quasi-static conditions, the hysteretic effect on the equilibrium position of the mass, caused by varying the external force, is easy to understand. A working model of the setup would not be hard to construct, so there is potential for its use as an introductory demonstration of hysteresis. It would be especially suitable due to the simplicity of physical concepts required to analyze the motion. This would be helpful for developing an intuitive understanding

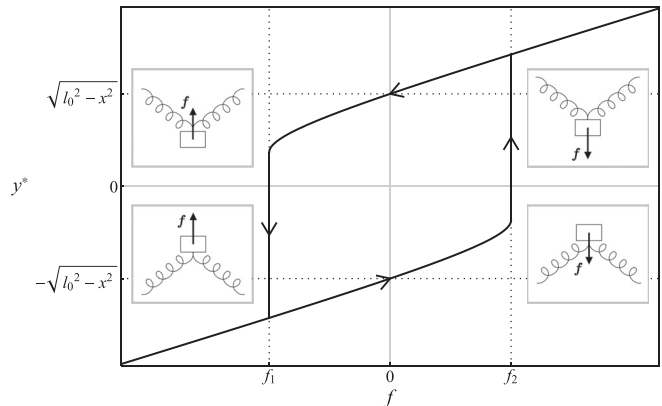


Fig. 5. Hysteresis curve. The (f, y^*) space is divided into four quadrants with differing signs of y^* and f , with a visual picture of the setup accompanying each quadrant.

of the sources of hysteresis in the system, and an appreciation for hysteresis as a general phenomenon that can present itself even in seemingly basic setups. The system is also suitable for use as an insightful quantitative exercise question for undergraduate physics students.

Interestingly, this system also turns out to be a mechanical analogue of some electronic switching devices. One such example is the pressure switch,¹³ whose open or closed state shows hysteretic dependence on the input pressure. Here, the external force f is analogous to the switch’s input pressure, while the two distinct spring configurations (V-shaped or inverted V-shaped) are analogous to the switch being open or closed. The two critical values f_1 and f_2 are also equivalent to the actuation points of the switch, and the hysteretic region $f_1 < f < f_2$ is similar to the switch’s deadband.

^aElectronic mail: chris97ong@gmail.com; Permanent address: 106B Faber Drive, Singapore.

¹M. Dawber, I. Farnan, and J. F. Scott, “A classroom experiment to demonstrate ferroelectric hysteresis,” *Am. J. Phys.* **71**(8), 819–822 (2003).

²J. A. Ewing, “On hysteresis in the relation of strain to stress,” in *British Association Reports* (1889), pp. 502–504.

³A. E. H. Love, *A Treatise on the Mathematical Theory of Elasticity*, 4th ed. (Dover, New York, 1944), p. 3.

⁴B. Denardo and R. Masada, “Rubber hysteresis experiment,” *Phys. Teach.* **28**(7), 489–491 (1990).

⁵*Demonstration Experiments in Physics*, edited by R. M. Sutton (McGraw-Hill, New York, 1938), pp. 287–290.

⁶D. C. Jiles and D. L. Atherton, “Theory of ferromagnetic hysteresis,” *J. Magnetism Magn. Mater.* **61**(1–2), 48–60 (1986).

⁷Yaakov Kraftmakher, “Hysteresis loops of a ferromagnet,” *Phys. Teach.* **43**(7), 439–441 (2005).

⁸P. Couletta, J. M. Gilli, M. Monticelli, and N. Vandenberghe, “A damped pendulum forced with a constant torque,” *Am. J. Phys.* **73**, 1122–1128 (2005).

⁹N. Alessi, C. W. Fischer, and C. G. Gray, “Measurement of amplitude jumps and hysteresis in a driven inverted pendulum,” *Am. J. Phys.* **60**, 755–756 (1992).

¹⁰L. N. Gonçalves, J. Fernandes, A. Ferraz, A. G. Silva, and P. J. Sebastião, “Physical pendulum model: Fractional differential equation and memory effects,” *Am. J. Phys.* **88**, 962–975 (2020).

¹¹C. L. Olson and M. G. Olsson, “Dynamical symmetry breaking and chaos in Duffing’s equation,” *Am. J. Phys.* **59**, 907–911 (1991).

¹²J. E. Berger and J. G. Nunes, “A mechanical Duffing oscillator for the undergraduate laboratory,” *Am. J. Phys.* **65**, 841–846 (1997).

¹³Bela G. Liptak, *Instrument Engineers’ Handbook*, 4th ed. (CRC Press, Boca Raton, 2003).